Journal Pre-proof

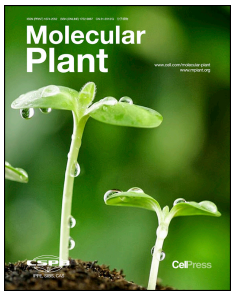

The transcription factor MYB44 suppresses starch synthesis to negatively regulate grain weight and yield in wheat and rice

Yunchuan Liu, Mingming Wang, Yaojia Wang, Haixia Liu, Wei Xi, David Seung, Xiaolu Wang, Lei Zhuang, Huifang Li, Tian Li, Hongxia Liu, Jian Hou, Xu Liu, Chenyang Hao, Xueyong Zhang

PII: S1674-2052(25)00182-0

DOI: https://doi.org/10.1016/j.molp.2025.06.007

Reference: MOLP 1926

To appear in: *MOLECULAR PLANT*

Received Date: 14 January 2025

Revised Date: 16 May 2025

Accepted Date: 13 June 2025

Please cite this article as: Liu Y., Wang M., Wang Y., Liu H., Xi W., Seung D., Wang X., Zhuang L., Li H., Li T., Liu H., Hou J., Liu X., Hao C., and Zhang X. (2025). The transcription factor MYB44 suppresses starch synthesis to negatively regulate grain weight and yield in wheat and rice. Mol. Plant. doi: https://doi.org/10.1016/j.molp.2025.06.007.

The transcription factor MYB44 suppresses starch synthesis to negatively regulate grain weight and yield in wheat and rice

Yunchuan Liu[1,2,3], Mingming Wang[2,3], Yaojia Wang[1,3], Haixia Liu[1,3], Wei Xi[1], David Seung[2], Xiaolu Wang[1], Lei Zhuang[1], Huifang Li[1], Tian Li[1], Hongxia Liu[1], Jian Hou[1*], Xu Liu[1*], Chenyang Hao[1*] and Xueyong Zhang[1*]

[1]State Key Laboratory of Crop Gene Resources and Breeding/National Key Facility for Crop Gene Resources and Genetic Improvement, Institute of Crop Sciences, Chinese Academy of Agricultural Sciences, Beijing, 100081, China.

[2]John Innes Centre, Norwich Research Park, Norwich, NR4 7UH, UK.

[3]These authors contributed equally to this article.

*Correspondence: Jian Hou (houjian@caas.cn), Xu Liu (liuxu03@caas.cn), Chenyang Hao (haochenyang@caas.cn) and Xueyong Zhang (zhangxueyong@caas.cn)

ABSTRACT

Starch is the principal storage compound in wheat grain, essential for flour quality and grain weight. In this study, we identified *TaMYB44*, an R2R3-MYB transcription factor gene, through a genome-wide association study. The *TaMYB44* homoeologs exhibited predominant expression in developing grains, with peak levels observed at 10 days after pollination. Functional analyses revealed that *TaMYB44* acts as a negative regulator of starch synthesis in the endosperm and limits grain size by repressing starch synthesis-related genes and modulating secondary metabolism. Knockout mutants of *TaMYB44* exhibited significantly increased starch accumulation, larger grain size, and enhanced yield stability across different growing environments. Additionally, we discovered that TaWDR1 interacts with TaMYB44, alleviating its repressive effects to restore starch synthesis and enhance grain weight. Moreover, we found that the functions of *MYB44* are partially conserved in both wheat and rice, underscoring its potential as a target for genetic improvement. Our findings provide valuable insights into the transcriptional regulation of starch synthesis and present genetic resources for improving grain yield in wheat and rice.

Key words: starch synthesis, grain weight, *TaMYB44*, transcription regulation, grain yield.

INTRODUCTION

Wheat (*Triticum aestivum* L.) is the most important cereal crop, supplying over one-fifth of the calories and protein for humans (FAO, 2023). Starch serves as the primary storage compound, comprising approximately 70% of wheat flour and plays a critical role in determining overall grain yield and flour quality (Shevkani et al., 2016). Enhancing starch synthesis through genetic or biotechnological approaches provides a viable strategy for improving wheat yield. A thorough understanding of the starch biosynthesis and its regulatory mechanisms is essential to achieve this goal.

In cereal crops, starch synthesis in the endosperm follows a conserved pathway, with sucrose produced during photosynthesis serving as the initial substrate (Emes, et al., 2003; Huang et al., 2021). Briefly, in developing grain endosperm, the sucrose is synthesized into starch through a series of enzyme-catalyzed reactions (Emes et al.,

2003; Chen et al., 2023). Disruption in the function of key enzymes or sugar transport proteins, such as sucrose synthase (Chourey et al., 1998; Deng et al., 2020; Shen et al., 2024), ADP-glucose pyrophosphorylase (Tsai and Nelson, 1966; Johnson et al., 2003), and Brittle1 (Shannon, et al., 1998; Wang et al., 2019) results in significantly impaired starch accumulation, ultimately leading to reduced grain weight. Although the biochemical steps of starch synthesis in cereal endosperm are relatively well characterized, the regulatory networks that orchestrate these enzymes at the transcriptional level during grain development are still not fully understood, especially in wheat.

Starch synthesis in the endosperm is governed by a complex and multilayered network that involves sugar and hormone signaling (Akihiro et al., 2005; Chen et al., 2011), microRNAs (Hu et al., 2021; Ma et al., 2023), protein modifications (Ma et al., 2021), and transcriptional regulation (Huang et al., 2021; Lopez-Gonzalez et al., 2019). Concerning transcription factors (TFs), one notable example is *TabZIP28*, the first TF demonstrated to positively regulate starch synthesis in wheat endosperm. Its overexpression led to a 4% increase in total starch content and a 5% increase in thousand grain weight (TGW) (Song et al., 2020). Similarly, *TabHLH95* is a positive regulator of starch synthesis, since knockout mutants exhibited reduced starch content and lower TGW (Liu et al., 2023b). Grain NAM, ATAF, and CUC (NAC) TFs, such as *TaNAC100* (Li et al., 2021), *TaNAC019* (Liu et al., 2020; Gao et al., 2021) and *TaNAC-A18* (Wang et al., 2023) also regulate the synthesis of starch and seed proteins in endosperm, mirroring the roles of NAC TFs (e.g. *OsNAC26*/*OsNAC20* (Wang et al., 2020), *OsNAC25* (Wang et al., 2024b), *ZmNAC128*/*130* (Zhang et al., 2019)) in maize and rice. Furthermore, the TaNF-YA3-D, TaNF-YB7-B, and TaNF-YC6-B trimer complex represses *TaNAC019*, further modulating starch synthesis (Chen et al., 2024). These numerous TFs implicated in starch synthesis demonstrate the complexity and multi-layered nature of transcriptional regulatory networks in wheat grain development. Therefore, identifying novel TFs that regulate starch synthesis in wheat endosperm remains crucial for further understanding these networks, which is important for enhancing wheat grain yield and quality.

In this study, we performed a genome-wide association study (GWAS) on a natural population of 145 sequenced wheat cultivars (Hao et al., 2020) and identified a MYB TF gene, *TaMYB44*, that associates with grain total starch content. Our results demonstrate that *TaMYB44* acts as a negative regulator of starch synthesis in the wheat endosperm. *TaMYB44* mutants exhibited a significant increase in total starch content and grain size, along with stable yield improvements across multiple growing environments. We demonstrated that *TaMYB44* negatively regulates starch synthesis by directly repressing the expression of starch biosynthesis genes and modulating secondary metabolic pathways. WD40 repeat proteins function as key regulatory scaffolds that influence protein-protein or protein-DNA interactions (Jain and Pandey, 2018). In this study, we discovered that *TaWDR1* interacts with *TaMYB44* and antagonizes its repressive function, thereby positively regulating grain weight. Furthermore, we revealed that *MYB44* also negatively regulates grain weight in rice, indicating a conserved function in both wheat and rice. Overall, our findings provide essential insights into the transcriptional regulation of starch synthesis in wheat and present valuable genetic resources for enhancing grain weight and endosperm starch accumulation in both wheat and rice.

RESULTS

GWAS for wheat grain total starch content

To explore the genetic basis of grain total starch content, we quantified the starch content in 145 wheat cultivars across two environments (Hao et al., 2020). A GWAS was performed using filtered single nucleotide polymorphisms (SNPs) from resequencing data to identify loci associated with total starch content. Under a mixed linear model with correction of the population structure and kinship ($P = 1.0\times10^{-5}$), we identified three major loci on chromosomes 1A, 4A and 7B associated with total starch content (Figure 1A, B). We focused on the linkage disequilibrium (LD) block on chromosome 4A *(qTSC4A*), which showed the lowest *P*-value and harbored ten high-confidence candidate genes (Figure 1C and Supplementary Table 1). Tissue-specific expression analysis using expVIP (Borrill et al., 2016) indicated that four of these genes are expressed in the developing grains, with *TraesCS4A02G006100* displaying grain-

specific expression (Figure 1D). Among the 145 cultivars, we identified five SNPs in its coding sequence (CDS), four of which led to amino acid changes, forming two haplotypes (Figure 1E). Accessions carrying *haplotype* (*Hap*) 2 exhibited higher total starch content than those with *Hap1* (Figure 1F). We refer to this gene as *TaMYB44*, as previously described by Wang *et al*. (2024).

TaMYB44 homoeologous lack introns (Supplementary Figure 1A) and are predominantly expressed in developing grains (peaking at 10 DAP in our data), with highest expression observed in *TaMYB44-D1* among the three homoeologous (Figure 1G and 1H). The full-length TaMYB44 exhibited no transcription activation activity in yeast (Supplementary Figure 1B). In wheat protoplast assays, TaMYB44 functions as a transcriptional repressor, in contrast to the strong activators VP16 and the GAL4-BD control, (Supplementary Figure 1C and 1D). Subcellular localization analysis showed that TaMYB44 is localized to the nucleus (Supplementary Figure 1E). Previous studies showed that *TaMYB44-D1* is co-expressed with genes related to storage protein, carbohydrate, and starch synthesis (Xiang et al., 2019; Gu et al., 2021). Collectively, these results reveal *TaMYB44* as a candidate gene for regulating starch accumulation in wheat endosperm.

TaMYB44 negatively regulates starch synthesis in wheat developing endosperm

To assess the functionality of *TaMYB44*, two independent triple knockout (KO) mutants were generated in wheat cultivars Fielder using CRISPR-Cas9, each carrying base deletions or insertions that cause frame shifts in all three homoeologous (Supplementary Figure 2A). Additionally, three overexpression (OE) lines driven by the *1Bx7* promoter (Geng et al., 2014) were developed in Fielder, showing significantly increased *TaMYB44* expression (Supplementary Figure 2B).

To investigate the role of *TaMYB44* in starch synthesis, we measured the total starch content in mature grains. Total starch content was significantly reduced in the *TaMYB44*-OE lines by 12.23% to 13.54%, while the *Tamyb44* triple KO lines showed an increase of nearly 12% compared to the WT (Figure 2A). Total starch content per grain followed the above trends in both the *TaMYB44*-OE and *Tamyb44* triple KO lines (Figure 2B). Furthermore, the total starch content under spring-sown condition

confirmed the stability of the starch accumulation conferred by *TaMYB44* (Supplementary Figure 2D). Supporting these findings, the *TaMYB44*-OE lines produced smaller and fewer starch granules at all developmental stages compared to the WT, whereas the *Tamyb44* triple KO lines displayed the opposite trend (Figure 2D and Supplementary Figure 2E). Consistently, in the mature endosperm, A-type starch granules were smaller in the *TaMYB44*-OE lines but larger in the *Tamyb44* triple KO lines (Figure 2E). These results together demonstrate that *TaMYB44* negatively regulates starch accumulation in developing wheat endosperm.

***TaMYB44* negatively regulates grain size and yield in wheat**

To evaluate the impact of *TaMYB44* on agronomic traits, we conducted field tests over two consecutive years. Compared to the WT, the grains of *Tamyb44* triple KO lines were noticeably larger, with significant increases in both grain length (GL) and grain width (GW), which contributes to a substantial increase in thousand grain weight (TGW) (Figure 2F-I and Supplementary Table 2). Additionally, the *Tamyb44-Abd* double mutant exhibited a significant increase in both grain size and TGW (Supplementary Figure 2F and Supplementary Table 2). In the single KO lines, *Tamyb44-ABd* showed a notable increase in grain size and TGW, whereas *Tamyb44-AbD* exhibited an increase in TGW without a significant change in grain size (Supplementary Figure 2F and Supplementary Table 2). Furthermore, we observed a negative correlation between the copy number of *TaMYB44* and TGW, suggesting a potential dosage effect (Supplementary Figure 2H). In contrast, *TaMYB44*-OE lines produced smaller grains with a more pronounced crease (Figure 2F). Specifically, all *TaMYB44*-OE lines consistently exhibited a significant reduction in GW across different environments, while GL was generally comparable to WT, with some lines even significantly larger. Consistently with the reduced GW, the TGW of the *TaMYB44*-OE lines was significantly lower than that of WT (Figure 2G-I and Supplementary Table 2). Furthermore, the *TaMYB44*-OE lines exhibited reduced grain yield, with per-plant decreasing by 21.5%-29.2% and plot yield by 8.58%-11.21% compared to WT. Conversely, the *Tamyb44* triple KO lines showed higher grain yield, with per-plant yield increasing by 15.3% and 24.8% and plot yield by 5.60% and 7.08%, respectively

(Figure 2J, K). These results were consistent over the two years (Supplementary Figure 2G and Supplementary Table 2). However, the double and single KO lines showed no significant difference compared to the WT (Supplementary Figure 2F and Supplementary Table 2).

In addition to affecting grain weight and yield, our results showed that other agronomic traits, such as plant height, tiller number (spike number per acre), and grain number per spike, exhibited minor and inconsistent changes across different years and growing conditions (Supplementary Figure 2G and Supplementary Table 2). Together, these findings reinforce that the grain-specific *TaMYB44* plays a crucial role in shaping grain-related characteristics.

TaMYB44 directly binds the promoters of *Sus1-A1*, *LD-B1*, and *TPP-D1* to repress their expression

To uncover the molecular mechanisms by which *TaMYB44* regulated starch synthesis and grain size, we integrated differentially expressed genes (DEGs) from transgenic versus WT comparisons with *Ta*MYB44 DNA-binding sites. Transcriptome analysis revealed 3,998 DEGs in *Tamyb44-abd* lines, of which 2,581 were upregulated. A total of 6,177 DEGs were identified in OE lines, with 3,215 downregulated (Supplementary Data 1). Gene Ontology (GO) term enrichment showed that the up-regulated DEGs in KO lines were enriched in processes like carbohydrate metabolism, trehalose biosynthetic, flavonoid biosynthesis, jasmonic acid signaling, and flavonol synthase activity (Figure 3C). Meanwhile, downregulated DEGs in OE lines were associated with the pathways such as UDP-glycosyltransferase activity, trehalose biosynthesis, sucrose synthase activity, and carbohydrate biosynthesis (Supplementary Figure 3D).

To identify the binding sites of TaMYB44, we employed a TaMYB44-Halo protein to affinity purify bound genomic fragments for sequencing. This analysis revealed numerous TaMYB44 binding regions, with 2.41% located in promoter regions and 3.18% near transcription termination sites (Supplementary Figure 3A, B). Motif enrichment analysis revealed that the TaMYB44 binding motif, [C/T]AAN[G/A][C/A/T][T/C/A], closely resembles the motif of subfamily IV of R2R3-MYB TFs (Jiang and Rao, 2020; Dai et al., 2022) (Figure 3A), a finding further validated by yeast one-hybrid (Y1H)

assays (Supplementary Figure 3E). By intersecting DEGs and DAP-seq data, we identified 45 overlapping genes as likely downstream targets of TaMYB44 (Figure 3B and Supplementary Figure 3C), including *TaTPP-D1*, *TaLD-B1*, and *TaLD-A1*, which are implicated in starch synthesis. Additionally, RT-qPCR analysis demonstrated that the expression of several starch synthesis-related genes, including *Sus1*, *Sus2*, *SBE2a*, and *BT1*, was significantly downregulated in OE lines (Supplementary Figure 3F). Conversely, the expression level of *Sus1* were significantly upregulated in *Tamyb44-abd* KO lines (Supplementary Figure 3G). Given the roles of sucrose synthase (Shen et al., 2024), LD (Li et al., 2019), and TPP (Liu et al., 2023a) in starch synthesis, we focused on *TaSus1-A1*, *TaLD-B1* and *TaTPP-D1* for further validation. DAP-seq peaks revealed that TaMYB44 directly binds to the promoter of *TaLD-B1* and *TaTPP-D1* in vitro (Figure 3D). Additionally, TaMYB44 binding motifs were identified in the promoters of *TaSus1* (Supplementary Figure 3H). EMSA using probes containing TaMYB44 binding motifs verified its interaction with the promoter regions of *Sus1-A1*, *LD-B1*, *TPP-D1*. These results were corroborated using Y1H assays (Figure 3E, F and Supplementary Figure 3I, K). Transient expression assays further demonstrated that TaMYB44 act as a transcriptional repressor for *LD-B1*, *Sus1-A1*, and *TPP-D1*, as shown by a reduced LUC/REN ratio in the presence of TaMYB44 (Figure 3G and Supplementary Figure 3L). Collectively, these results establish that TaMYB44 directly binds to and represses starch synthesis-related genes, including *LD-B1*, *Sus1-A1*, and *TPP-D1*.

The *TaMYB44-TaUGT83A1* module regulates starch synthesis and grain weight

Among the 45 overlapping genes, *TaUGT83A1-B1* and *TaUGT83A1-D1* were homoeologous and exhibited significantly altered expression levels in transgenic lines compared to the WT (Supplementary Figure 3C). DAP-seq revealed that TaMYB44 directly binds to the promoters of *TaUGT83A1-B1* and *TaUGT83A1-D1* (Figure 3D), a result confirmed by EMSA and Y1H assays (Figure 3E, F). Furthermore, LUC activity assays demonstrated that TaMYB44 represses the expression of *TaUDT83A1-B1* and *-D1* (Figure 3G).

In rice, *UGT83A1* is a critical regulator of grain size, controlling metabolite flow and

hormone synthesis (Dong et al., 2020). RNA-seq analysis of *Tamyb44* triple KO grains revealed a significant increase in JA signaling-related genes (Figure 4A), alongside elevated levels of JA and JA derivatives (Figure 4B). Additionally, metabolites such as flavonoids, lipids, and trehalose were notably altered in *Tamyb44* triple KO developing grains (Supplementary Figure 4 and Supplementary Data 2), suggesting that *TaMYB44* may influence secondary metabolism and hormones by regulating *TaUGT83A1* expression, thereby impacting starch synthesis and grain weight.

To investigate the function of *TaUGT83A1* in wheat, two EMS mutants in the durum wheat (cv. Kronos) background (Uauy et al., 2009) were analyzed (Figure 4C). Two mutants showed significantly lower total starch content (Figure 4E). Consistently, *Taugt83a1* mutants produced smaller grains (Figure 4D). Statistical analysis showed significant decreases in GL and GW, resulting in a sharp reduction in TGW (Figure 4F-H). Consequently, grain yield per plant was significantly lower in the mutants compared to WT (Figure 4I). Taken together, these results demonstrate that *TaUGT83A1* acts as a downstream target of TaMYB44 and positively regulates starch synthesis and grain weight, forming a genetic mechanism that controls grain weight and yield.

TaMYB44 interacts with TaWDR1 to form a nuclear complex

MYB transcription factors in plants typically form dimers or trimers to regulate gene expression (Stracke et al., 2001; Dubos et al., 2010). Through two-hybrid (Y2H) screening, we identified 18 potential proteins that interact with TaMYB44 (Supplementary Table 3). Notably, we discovered a WD40 repeat protein, TraesCS6D02G265000, named TaWDR1, which may function similarly to other WD40 proteins by forming MYB-bHLH-WD40 (MBW) complexes with MYB and bHLH TFs, thereby influencing their regulatory activities (Ramsay and Glover, 2005).

expVIP (Borrill et al., 2016) analysis revealed that *TaWDR1* is expressed in all examined tissues (Supplementary Figure 5A), and colocalized with TaMYB44 in wheat protoplasts (Figure 5A). Y2H assays confirmed that TaMYB44 physically interacts with TaWDR1 (Figure 5B). This interaction was further validated by luciferase complementation imaging (LCI) (Supplementary Figure 5B), and through bimolecular fluorescence complementation (BiFC), which localized the interaction specifically to

253 the nucleus (Supplementary Figure 5C). Co-immunoprecipitation (Co-IP) assays
254 confirmed the interactions at the protein level (Figure 5C). These findings suggest that
255 TaWDR1 and TaMYB44 form a nuclear complex, potentially regulating starch
256 synthesis and grain weight in wheat.

257 **TaWDR1 attenuates the negative effects of TaMYB44 on starch synthesis and**
258 **grain weight**

259 We investigated the effects of the interaction between TaMYB44 and TaWDR1 on
260 starch synthesis and grain weight by integrating molecular assays with genetic
261 approaches. To assess the effect of TaWDR1 on the activity of TaMYB44, we conducted
262 LUC reporter assays in wheat protoplasts (Supplementary Figure 6A). Co-expression
263 of *p35S::REN-pSus1-A1* (or *pLD-B1* or *pTPP-D1* or *pUGT83A1-B1/-D1*)*::LUC* with
264 *p35S::TaMYB44* resulted in a significant reduction in LUC activity compared to the
265 control (Supplementary Figure 6C). Meanwhile, co-expression with *TaWDR1* exhibited
266 no significant change in the LUC/REN ratio compared to the control (Supplementary
267 Figure 6C). Notably, co-expression of *TaWDR1* with *TaMYB44* led to a pronounced
268 restoration of LUC activity, with *pLD::LUC*, *pTPP::LUC*, and *pSus1::LUC* showing
269 no significantly differences from the control, whereas *pUGT83A1-B1/-D1::LUC*
270 remained lower than the control (Supplementary Figure 6C). Despite these findings,
271 EMSA results revealed that TaWDR1 does not directly bind to the promoters of
272 TaMYB44 downstream genes, nor does it significantly alter TaMYB44's DNA-binding
273 affinity (Supplementary Figure 6D). Consistently, the expression levels of the
274 aforementioned genes in *TaWDR1*-OE developing grains showed no significant
275 differences compared to those in WT (Supplementary Figure 6 B and 6E). However, in
276 F3 generation of *TaWDR1*-OE and *TaMYB44*-OE, the expression of these genes was
277 significantly higher compared to the *TaMYB44*-OE lines, reaching the levels observed
278 in WT (Supplementary Figure 6E). These findings indicate that TaWDR1 can attenuate
279 the negative regulatory effect of TaMYB44 on its downstream targets.

280 To elucidate the biological function of *TaWDR1*, we generated *TaWDR1*-OE lines in
281 the Fielder wheat (Figure 5E). The *TaWDR1*-OE lines showed increased starch
282 accumulation in the developing endosperm and higher total starch content levels in the

283 mature grains compared to the WT, with *TaWDR1*-#3 displaying a statistically
284 significant difference (Figure 5F, 5I). Correspondingly, the *TaWDR1*-OE lines
285 developed larger grains than the WT (Figure 5D). Specially, the GW of *TaWDR1*-OE
286 lines were significantly increased, resulting in a significant increase in TGW (Figure
287 5G, 5H and Supplementary Table 4).
288 To evaluate the genetic interaction between *TaWDR1* and *TaMYB44*, we crossed their
289 respective OE lines and self-pollinated the F_3 generation for phenotypic analysis. TEM
290 analysis showed that starch granules accumulation in the endosperm of F_3 plants was
291 comparable to WT and significantly more than that observed in *TaMYB44*-OE (Figure
292 5I). Furthermore, the F_3 plants restored total starch content levels to those of WT, but
293 their levels remained slightly lower than in *TaWDR1*-OE lines (Figure 5K). Accordingly,
294 GW and TGW of F_3 generations also nearly restored to WT levels, showing no
295 significant differences from WT under spring-sown single-row planting conditions.
296 Notably, the genetic interaction was consistent regardless of the direction of the crosses
297 (Figure 5L, 5M and Supplementary Table 5). These results demonstrate that *TaWDR1*
298 functions as a positive regulator of starch synthesis and grain weight by mitigating the
299 negative regulatory effects of *TaMYB44* on downstream targets.
300 ***MYB44* is functionally conserved in rice and wheat**
301 To determine whether the function of *MYB44* is conserved in cereals, we grew three
302 *p1Bx7::TaMYB44* rice lines in the field for phenotypic analysis (Supplementary Figure
303 7A, C). Compared to KitaaKe, the *p1Bx7::TaMYB44* lines exhibited approximately 10%
304 less total starch, nearly 4% less amylose, but significantly higher protein content
305 (Figure 6A-C). The mature grains of *p1Bx7::TaMYB44* rice displayed a chalky, starchy
306 endosperm with loosely arranged, spherical starch granules (Figure 6D). Semi-thin
307 sections and TEM analysis further revealed that *p1Bx7::TaMYB44* rice produced fewer,
308 smaller, and more loosely packed starch granules in the developing endosperm
309 compared to KitaaKe (Figure 6E, F). Consistent with changes in starch content, the
310 TGW of *p1Bx7::TaMYB44* rice was significantly reduced, while GW remained
311 comparable to KitaaKe (Figure 6G and Supplementary Figure 7E). Interestingly, GL of
312 *p1Bx7::TaMYB44* rice lines displayed environmental variability, with a significant

decrease observed in Beijing, but a slight, non-significant increase in Sanya (Supplementary Figure 7B, D). Additionally, the grain yield per plant of *p1Bx7::TaMYB44* rice lines was significantly reduced compared to Kitaake, with stable effect across different environments (Figure 6H).

Transcriptome analysis revealed that the down-regulated DEGs in *p1Bx7::TaMYB44* rice were enriched in pathways related to starch and sucrose metabolism, plant hormone signal transduction, flavonoid biosynthesis, and biosynthesis of secondary metabolites (Figure 6I and Supplementary Data 3), consistent with the results in wheat.

We also cloned *OsMYB44* (*Os01g0977300*) and performed preliminary functional analysis. It encodes a nuclear-localized protein with no autoactivation activity (Supplementary Figure 8A, B). To explore its biological function, we generated KO mutants and *p1Bx7::OsMYB44* lines in the KitaaKe (Supplementary Figure 8C, D). Like that found in wheat, the *p1Bx7::OsMYB44* lines exhibited a significant reduction in TGW, whereas the *Osmyb44*-KO mutants showed a marked increase (Supplementary Figure 8G, K). The *Osmyb44* mutants showed a significant increase in both GL and GW (Supplementary Figure 9L, M). The GW of *p1Bx7::OsMYB44* lines was similar to that of KitaaKe, while the GL displayed an increase, which was significant in line *p1Bx7::OsMYB44*#3 under Sanya conditions and all lines under Beijing conditions (Supplementary Figure 8H, I, L and M). The grain yield per plant of was significantly reduced in *p1Bx7::OsMYB44* lines but increased in *Osmyb44*-KO mutants compared to WT (Supplementary Figure 8J, 10N). Furthermore, the total starch content of *p1Bx7::OsMYB44* grains was generally lower, but significant reduction was only observed in line *p1Bx7::OsMYB44*#2 under Sanya conditions and line *p1Bx7::OsMYB44*#3 under Beijing conditions (Supplementary Figure 8O, Q). Starch content per grains was significantly reduced in *p1Bx7::OsMYB44* lines compared to KitaaKe (Supplementary Figure 8P). In comparison, although the total starch content of *Osmyb44* mutant line increased, the difference compared to WT was not statistically significant (Supplementary Figure 8Q). Furthermore, RT-qPCR results showed that the expression levels of starch synthesis-related genes, including *LD*, *Sus1*, *Sus3*, *HXK4*, *UGT83A1*, *AGPL1*, and *AGPS2b*, were downregulated in *p1Bx7::OsMYB44* rice lines,

consistent with the findings in *p1Bx7::TaMYB44* rice lines (Supplementary Figure 9). Taken together, these results suggest that *MYB44* is involved in the regulation of starch biosynthesis and grain weight, pointing to a potentially conserved role in wheat and rice.

TaMYB44-A1-Hap2 is a favorable haplotype associated with higher grain weight and undergone positive selection during wheat breeding in China

To evaluate the breeding relevance of *TaMYB44*, we analyzed its haplotype variation in both Chinese and global wheat accessions. Using 145 Chinese wheat accessions along with resequencing data from 1,020 global accessions (Cheng et al., 2024), we found no SNP variation within the *TaMYB44-B1* gene region. Although three haplotypes were identified *TaMYB44-D1*, *Hap2* and *Hap3* were present in only 16 and 31 accessions, respectively, and no variation was detected in the 145 Chinese accessions, leading us to focus on *TaMYB44-A1* for further analysis.

In the global panel, *TaMYB44-A1* exhibited notable haplotype diversity. After excluding those with missing genotype (i.e., './.' sites), eight distinct haplotypes were identified, with *Hap1* and *Hap2* being the most prevalent (Supplementary Figure 10A). The remaining six haplotypes, each found in less than 2% of the population, were excluded from further analysis. Based on the SNP_593, we developed a dCAPS marker to distinguish the two haplotypes in a panel of 348 Chinese modern cultivars and 157 Chinese landraces (Supplementary Figure 10B). Association analysis revealed that *TaMYB44-A1-Hap2* was significantly associated with higher TGW in both landrace and modern cultivar populations (Supplementary Figure 10C and 10D). Moreover, the frequency of *TaMYB44-A1-Hap2* increased from 9.677% in the landraces to 43.69% in modern cultivars, indicating that it underwent selected during Chinese breeding process (Supplementary Figure 10F and 10G). Although the frequency of the *TaMYB44-A1-Hap2* is increasing in China, its global prevalence remains low, with occurrences of only 4.15% in Europe, 13.83% in North America, 21.28% in Australia, 22.07% in Russia, and 28.30% in CIMMYT (Supplementary Figure 10H), highlighting its potential for improvement in other regions.

To explore the functional basis underlying haplotype difference, we examined

TaMYB44 expression in developing grains from the two haplotypes. *Hap2* showed lower expression levels compared to *Hap1*, with transcript abundance in three *Hap2*-carrying accessions significantly lower relative to the Chinese Spring, a *Hap1* carrier (Supplementary Figure 11A). Furthermore, transient expression assays were conducted to evaluate the regulatory activity of the two haplotypes on downstream genes, revealing no significant differences between the two haplotypes (Supplementary Figure 11B and 11C). Overall, *TaMYB44-A1-Hap2* represent a favorable haplotype associated with higher grain weight and undergone positive selection during wheat breeding in China.

DISCUSSION

Understanding the regulatory network of starch synthesis in wheat endosperm is critical for enhancing wheat quality and grain yield. In this study, we present persuasive evidence that *TaMYB44* acts as a negative regulator of starch synthesis in wheat endosperm through three distinct mechanisms, thereby reducing grain weight and yield (Figure 7). While prior studies have hinted a link between *TaMYB44* and starch synthesis (Xiang et al., 2019; Gu et al., 2021), our findings provide a more detailed and experimentally supported model.

The first and most straightforward mechanism involves the downregulation of genes directly involved in starch synthesis. Specifically, several genes, including *Sus1*, *LD*, *ISA1*, *Sus2*, and *BT1*, were significantly downregulated in *TaMYB44*-OE lines. We demonstrated that TaMYB44 directly binds to the promoters of *TaSus1-A1* and *TaLD-B1*, repressing their expression and thus reducing starch accumulation. Notably, previous works have shown that *Sus1* haplotypes are associated with grain weight and *Tasus1* mutants produce smaller grains (Hou et al., 2014; Shen et al., 2024). *Sus1* expression is therefore expected to have major effects on grain weight. Likewise, *LD* expression may also contribute to these effects, given its partial overlap functions with *ISA1* in starch synthesis (Fujita et al., 2009). In sorghum, allelic variation in *LD* is associated with altered starch content, (Li et al., 2019), further supporting its importance.

Second, TaMYB44 interferes with the trehalose-6-phosphate (T6P) signaling pathway,

a key regulator of sucrose utilization and carbon partitioning (Elbein et al., 2003; Paul et al., 2020; Fichtner and Lunn, 2021). Our results show that TaMYB44 represses *TaTPP-D1* expression, reducing trehalose accumulation and consequently impeding starch synthesis. This aligns with findings that *Tatpp-7A* mutants exhibit lower trehalose, along with decreased total starch content and grain weight in wheat (Liu et al., 2023a). The third mechanism involves effects on starch and grain development through secondary metabolite biosynthesis and hormonal pathways. R2R3-type MYB TFs are well-known regulators of flavonoid biosynthesis and hormone signaling pathways (Jiang and Rao, 2020; Wang et al., 2024a). Transcriptomic data from *Tamyb44*-KO lines revealed upregulation of genes enriched in flavonoid biosynthesis and Jasmonic acid (JA) signaling pathways. JA, a hormone typically involved in stress response (Ghorbel et al., 2021), has also been reported to positive regulator of gain width and grain weight (Chen et al., 2020; Mehra et al., 2022; Niaz et al., 2023). Although TaMYB44 does not directly regulate JA-related genes, it directly represses *TaUGT83A1-B1* and *-D1*, which encode UDP-glycosyltransferases (UGTs) known to regulate secondary metabolites, hormone homeostasis and grain size (Ross et al., 2001; Ostrowski and Jakubowska, 2014; Dong et al., 2020; Cao et al., 2024). Supporting this model, *Taugt3a1* mutants exhibited reduced starch content, smaller grain size, and grain weight, suggesting that TaMYB44 may indirectly modulate JA accumulation by regulating secondary metabolite synthesis, such as flavonoids, via *TaUGT83A1*. Overall, this study introduces *TaUGT83A1* as a novel component of the regulatory network governing starch synthesis in wheat and offers new insights into improving grain weight and yield. Consistent with its transcriptional repressor role, TaMYB44 exhibited transcriptional repressive activity in both yeast and wheat protoplasts. *Tamyb44* triple KO mutants displayed increased starch content and grain weight, supporting that *TaMYB44* functions as a negative regulator. Moreover, a negative correlation between grain weight and *TaMYB44* gene dosage was observed, strengthening this conclusion. Although genetic complementation evidences are still needed, the phenotypic data strongly support the conclusion that *TaMYB44* functions as a negative regulator of starch synthesis and grain weight.

Natural variation in *TaMYB44-A1* underscores its importance in wheat breeding. Two major haplotypes, *Hap1* and *Hap2*, are associated with significant and stable differences in grain weight across both Chinese modern cultivars and landraces. *Hap2*, which exhibits lower expression in developing grains, is association with higher TGW. Although four non-synonymous SNPs were identified in the *TaMYB44-A1* coding region, transient assays revealed no significant differences between the two haplotypes in regulating the downstream genes. Therefore, we speculate that the differences in grain weight and starch content between the two haplotypes appear to be caused by difference in *TaMYB44* expression driven by promoter variation. Future work involving transgenic overexpression of each haplotype will be essential to confirm function variation and inform marker-assisted selection strategies.

MYB TFs generally form complexes with WD40 repeat proteins and bHLH TFs to regulate plant growth and development (Ramsay and Glover, 2005). In this study, we found that TaMYB44 interacts with the WD40-repeat protein TaWDR1. Notably, TaWDR1 neither binds to the downstream genes of *TaMYB44* nor interfere with TaMYB44's DNA binding, indicating that it does not act through competitive inhibition. However, when *TaWDR1* and *TaMYB44* are co-expressed—either via transient expression systems or stable dual overexpression in developing wheat grains—*TaWDR1* consistently mitigates the transcriptional repression mediated by *TaMYB44*. The restoration of starch content and grain weight in the *TaWDR1* and *TaMYB44* double OE lines further supports the antagonistic role of *TaWDR1* in modulating *TaMYB44*-mediated repression. In addition to TaWDR1, protein interaction assays identified multiple TaMYB44-interacting proteins, including TabHLH95, a positive regulator of starch synthesis (Liu et al., 2023), as well as TaMYB44 itself, suggesting that TaMYB44 may form oligomeric or multiprotein complexes with other transcription or co-factors to exert its regulatory functions. Given that WD40-repeat proteins often act as scaffolds that facilitate or weaken protein–protein and protein–DNA interactions (Ramsay and Glover, 2005), we propose that TaWDR1 may modulate TaMYB44 regulatory activity by altering its conformation or hindering co-repressors recruitment. Future dissection of these interactions may provide opportunities to manipulate this

network for wheat improvement.

The starch biosynthesis pathway is largely conserved among cereal crops (James et al., 2003); however, the extent to which upstream TFs function similarly across cereals remains unclear. Key regulators such as OsbZIP58 and OsRSR1 have demonstrated conserved roles in cereals (Fu and Xue, 2010; Kang et al., 2013; Kawakatsu et al., 2009; Zhang et al., 2016). In this study, we reveal that *TaMYB44* negatively regulates starch synthesis and grain weight in wheat, and that this function appears to be partially conserved in rice through its homolog *OsMYB44*. Overexpressing either *TaMYB44* or *OsMYB44* in rice significantly reduced grain weight, which was accompanied by the downregulation of multiple starch biosynthesis-related genes, including *AGPL1*, *AGPS2a*, *SUS1*, *LD*, *UGT83A1*, and *SBEIIb* in rice. Although expression data from *Osmyb44*-KO lines are currently lacking, our findings suggest that *MYB44* orthologs may negatively regulate starch accumulation by modulating the expression of starch biosynthesis-related genes. Interestingly, despite the pronounced changes in grain weight, both OE and KO of *OsMYB44* led to only minor alterations in starch content. This observation may indicate functional redundancy or compensatory regulation by other TFs in rice. Collectively, our results support a model in which *MYB44* plays a conserved role in starch biosynthesis in wheat and rice. While its core regulatory function appears maintained, the magnitude and specificity of its effects are shaped by species-specific genetic and molecular contexts. Future research should aim to identify new targets of *MYB44* and elucidate its interaction network—including both synergistic and antagonistic partners—to better understand its role in coordinating starch metabolism and grain development in cereal crops.

In summary, our study establishes *TaMYB44* as a crucial TF in regulating starch synthesis in wheat endosperm through multiple pathways. The interaction between TaWDR1 and TaMYB44 antagonizes the latter's effects, facilitating starch accumulation. Moreover, our findings suggest that *MYB44* is functionally conserved in wheat and rice and holds potential for genetic enhancement.

METHODS

Plant materials and cultivation

Wheat (cv. Chinese Spring) was grown in a greenhouse under 16 h light / 8 h dark photoperiod, and tissues were sampled at various developmental stages for expression pattern analysis. Seedling were planted in plug trays and grown in complete darkness until it had two full leaves and was then used to extract protoplasts.

For the phenotypic evaluation, transgenic wheat lines and Fielder (WT, carrying *TaMYB44-A1-Hap2* and *TaMYB44-D1-Hap1*) were grown under natural conditions in experimental fields in Shunyi, Beijing (116° E, 40° N) in 2022 and 2023. Specifically, WT, *Tamyb44*-KO, *TaMYB44*-OE, *TaWDR1*-OE lines, as well as the F_3 progeny from crosses between *TaMYB44*-OE and *TaWDR1*-OE, were planted in two-meter-wide plots consisting of six rows, with 30 cm spacing between rows and 20 seeds per row. The growing seasons ranged from mid-October to mid-June for winter sowing, and from mid-March to early July for spring sowing. Each line was planted with three replicates. Additionally, the *Tamyb44*-KO, *TaMYB44*-OE and WT were sown at a seeding density of 3.0 million seeds per hectare in 12 m^2 plots, with six replicates in 2022 and three replicates in 2023. To measure the grain yield per hectare, in 2022, two 0.66 m^2 subplots with uniform growth were selected within each plot for manual harvested. The grain yield from these subplots was measured and converted to yield per hectare. In 2023, the entire plot was harvested mechanically, and the total yield was measured and converted to yield per hectare. The *Taugt83a1* mutants were grown under natural conditions in experimental fields in Shunyi, Beijing (116° E, 40° N) from mid-March to early July 2022.

For transgenic rice phenotypic analysis, the *p1Bx7::TaMYB44* rice and KitaaKe were cultivated in experimental fields in Shunyi, Beijing (116° E, 40° N) from June to October 2022, and in Sanya (109° E, 18° N) from December (2022) to April (2023). The T_1 generation *p1Bx7::OsMYB44* rice lines and KitaaKe were cultivated in experimental fields in Sanya (109° E, 18° N) from December to April in 2022-2023. Additionally, KitaaKe, *p1Bx7::OsMYB44* (T_2 generation) and *Osmyb44*-KO lines were grown in experimental fields in Shunyi, Beijing (116° E, 40° N) from June to October in 2023. Rice seedlings were planted in 1*1.5 m^2 plots with four rows per plots, and 15 plants per row. Each line was planted with two replicates.

Agronomic traits, including plant height, spike length, grain number per spike, TGW, GL, GW, grain yield per plant and total starch content, were assessed on a single-row grown conditions plant basis.

Genome-wide association study

A panel of 145 re-sequenced wheat accessions (Hao et al., 2020) was utilized to identify genes associated with total starch content. The plant materials were planted in Xinxiang (113° E, 35° N), Henan, and Shunyi (116° E, 40° N), Beijing, during the 2019 and 2020 growing season, respectively. Each plot measured 1.2 m in width, with a row spacing of 30 cm and 20 seeds sown per row. Following harvest, total starch content was measured and subsequently employed for GWAS.

This study applied the mixed linear model (MLM) with the correction of population structure (Q) and kinship (K) in GEMMA (Genome-wide efficient mixed-model association) software (Zhou and Stephens, 2012) to conduct GWAS, and took $P = 1.0 \times 10^{-5}$ as the threshold value to determine the significance of the association between SNP markers and target traits. The analysis utilized SNPs derived from whole-genome resequencing data, which are accessible under the accession number PRJNA597250 in the NCBI database (Hao et al., 2020).

Plasmids construction and plant transformation

For *TaMYB44*, we generated OE plants in rice and wheat, and KO in wheat. The *Ubiquitin* promoter was used to generate overexpression of the constitutively expressed gene *TaWDR1*, while the *1Bx7* promoter was used for overexpression of the grain-dominantly expressed genes *TaMYB44* and *OsMYB44*. To generate OE plants, the open reading frame (ORF) of *TaMYB44-D1* was amplified from cDNA of developing grains of Chinese Spring wheat and cloned into the modified pCAMBIA2300 vector which driven by *1Bx7* promoter. To generate *Tamyb44*-KO mutants in Fielder wheat, we designed a common sequence (5'-CCAGCTCAGCCCGGCCGTGCAGC-3') that targets *TaMYB44* homologous for CRISPR/Cas9-mediated KO. This sequence was cloned into pBUE411 vector. In addition, to form *TaWDR1-D1*-OE wheat, we cloned the coding sequence (CDS) of *TaWDR1-D1* into pWMB110 vector under control of the ubiquitin promoter. To generate *OsMYB44*-OE plants, the CDS of *OsMYB44* was

cloned into pCAMBIA2300 vector under control of the *1Bx7* promoter. For *Osmyb44*-KO, a special sequence (5'-CATCATCAGCGGCGCCATCCCGG-3') was utilized as the sgRNA for CRISPR/Cas9-mediated gene knockout, which was constructed into the pBUE411 vector. Transgenic plants were generated through *Agrobacterium tumefaciens* mediated transformation, using the Fielder variety for wheat and the Kitaake variety for rice as the transformation recipients.

RT-qPCR and RNA-seq analyses

Total RNAs were extracted from wheat and rice tissues using the Plant RNA reagent and the cDNA was synthesized with the Superscript IV Kit (Invitrogen, USA). RT-qPCR was performed on a Roche instrument, and *Actin* was used as the internal reference to calculate the expression level of target genes using $2^{-\Delta\Delta Ct}$ methods. Each experiment was performed with three biological replicates. All primers used here are listed in Supplemental Data 4.

For RNA sequencing, developing grains at 12 DAP of WT and *TaMYB44* transgenic (OE and KO) lines were collected to construct the sequencing library. Three biological replicates were performed for each genotype. The clean reads were mapped to the latest version of the Chinese Spring genome (IWGSC RefSeq v2.1) (Zhu et al., 2021). The DESeq2 R package was utilized to analyze differential gene expression (Love et al., 2014), with a significance threshold set at *P*-value < 0.05 and |log2 Foldchange| >=0. Gene Ontology (GO) term enrichment analysis was conducted using agriGO v2.0 (Tian et al., 2017).

In rice, developing grains at 8DAP from the KitaaKe and *TaMYB44*-OE were utilized for transcriptome analysis, as previously described (Niu et al., 2020).

Metabolomics and endogenous JA content measurements

Grains from WT (Fielder) and *Tamyb44*-KO plants were collected at 12 and 16 DAP and frozen in liquid nitrogen. For metabolomics analysis, the grains were ground and extracted with 70% methanol. The resulting supernatant was centrifuged and filtered through a microporous membrane (0.22 μm size) before being analyzed using UPLC-MS/MS. Data analysis was conducted by Metware Biotechnology (Wuhan, China). To measure the endogenous jasmonic acid (JA) content, 100 mg of the ground sample was

prepared for reaction according to established protocols. The JA content was then quantified using LC-MS/MS, with analysis performed by Metware Biotechnology.

Protein subcellular localization

The ORF of *TaMYB44* and *OsMYB44* without the termination codon, were amplified and cloned into the pJIT163-GFP to fuse with green fluorescence protein (GFP). The CDs of *TaWDR1-D1* was fused to red fluorescence protein (RFP). Protoplasts were isolated from the leaves of one-week-old wheat seedlings and then used for the transient expression of these constructs. The fluorescence signal was analyzed by confocal microscopy (LSM880; Carl Zeiss, Germany) after 16 h of culture under 24℃, dark condition.

Yeast assays

The ORF of *TaMYB44-D1* was cloned into the pGBKT7 vector and then transformed into Y2H-gold yeast cells as bait. The bait was mated with the grain library (Liu et al., 2020) to identify candidate interacting proteins. For the yeast two hybrid assay, the ORF of *TaMYB44-D1* and *TaWDR1-D1* were fused with GAL4 activation domain (AD) and -binding domain (BD), respectively, and co-transformed into Y2H-glod cells. The cells were incubated on SD/-Trp/-Leu/-His/-Ade medium to verify interactions.

For the yeast one hybrid assay, the ORF of *TaMYB44-D1* was constructed in the pB42AD vector, while the core promoters of downstream targets were cloned into the pLacZi vector as the reporters. The resulting constructs were co-transformed into EGY48 yeast cells, and interaction were detected on the SD/-Trp/-Ura-X-gal medium.

LCI and BIFC assays

For the LCI assay, the CDS of *TaMYB44-D1* and *TaWDR1-D1* were cloned into the 35S-nLUC and 35S-cLUC vectors, respectively. The resulting constructs were then transformed into *Agrobacterium* strain GV3101. Transformed cells were cultured in Luria-Bertani liquid medium containing Kanamycin and Rifampicin until they reached an OD_{600} of 1. The cells were then re-suspended in a suspension buffer (50 mL total value containing 0.5 mL 1M MES, 0.5 mL 1M $MgCl_2$, 50 μL 0.2M AS) and subjected to a one-hour dark treatment. After mixing in equal proportions, the cells were infiltrated into the leaves of *N. benthamiana*. The plants were subsequently grown

under photoperiodic conditions of 16 hours of light and 8 hours of darkness for two days. The leaves were evenly coated with firefly luciferase substrate and allowed to react in dark for two minutes. The Nightshade LB985 imaging system (Berthold Technologies, Germany) was employed to detect the fluorescent signal.

For BIFC assay, the ORFs of *TaMYB44-D1* and *TaWDR1-D1* were fused with C- and N-terminus of yellow fluorescence protein (YFP) to generate TaMYB44-cYFP and TaWDR1-nYFP, respectively. The resulting constructs were transformed into *Agrobacterium* strain GV3101 and then infiltrated into the leaves of *N. benthamiana* plants. The YFP signal was detected using a laser confocal microscope (LSM880; Carl Zeiss, Germany).

LCI experiments were conducted with GFP-nLUC and GFP-cLUC vectors as controls, and BIFC experiments used empty vectors as controls. Each experiment for both LCI and BIFC was performed no less than three times.

CO-IP assay

The CDS of *TaMYB44-D1* and *TaWDR1-D1* were amplified and fused with *3×Flag* and *GFP*, respectively. The indicated constructs were transformed into the *Agrobacterium* strain GV3101 and co-infiltrated into the leaves of *N. benthamiana*. Immunoprecipitation and western blotting were conducted according to previously reported methods (Li et al., 2023). Each experiment was performed in triplicate to ensure the reliability of the results.

DNA affinity purification sequencing

Genomic DNA from Chinese Spring was extracted and fragmented into 600-800 bp segments using sonication to create the input library. The ORF of *TaMYB44-D1* was fused with HALO and then expressed *in vitro* using the TnT SP6 High-Yield Wheat Germ Protein Expression System (Promega, USA), following the manufacturer. HALO beads were used to enrich and purify the TaMYB44-HALO protein. Next, a sequencing DNA library was prepared as described by Pei *et al*., (2023), and sequenced on a NextSeq500 platform. Data analysis and processing followed methods previously reported (Pei et al., 2023). All primers used for DAP-seq are listed in the Supplementary Data 4.

EMSA

The CDS of *TaMYB44-D1* was inserted into the pMAL-c2x vector, fused with Maltose Binding Protein (MBP), and transfected into Escherichia coli strain BL21 (DE3). The cells expressing the TaMYB44-MBP fusion and MBP-tag were cultured in 300 mL of medium and induced with 0.5 mM isopropyl β-D-1-thiogalactopyranoside (IPTG) at 16°C for 14 hours. Harvested cells were lysed by sonication at -4°C, and the supernatant was incubated with 500 μL of Amylose Resin High Flow (New England Biolabs, USA) to purify the TaMYB44-MBP fusion protein and MBP-tag. Probes containing MYB-binding motif were synthesized and biotinylated at the 3' end. EMSA was performed using the LightShift Chemiluminescent EMSA kit (Thermo Fisher Scientific, USA). Probe sequences are listed in the Supplementary Data 4.

Dual-luciferase reporter assay

The approximately two kb promoter fragment of downstream genes was amplified from Chinese Spring and cloned into the pGreenII-0800 vector to construct the reporter. The ORFs of *TaMYB44* and *TaWDR1-D1* were cloned into the 35S-GAL4DB-NOS vector to serve as the effector constructs, while the 35S-GAL4DB-NOS vector alone was used as a control. Reporter and effector constructs were co-transformed into wheat protoplasts at a 1:3 or 1:3:3 ratio, and incubated in the dark at 24°C for 16 hours. LUC and REN activities were measured using the dual-luciferase reporter assay system (Promega, USA). Each experiment was conducted at least five times.

Microscopy assay

For transmission electron microscopy (TEM) analysis, developing grains of wheat and rice were sampled and fixed in sodium cacodylate buffer containing 2.5% glutaraldehyde. After fixation, the samples were dehydrated with a gradient of alcohol and then embedded using the Technovit 7100 kit (Technovit, Germany). Thin sections of the embedded samples were then prepared with a Leica EM UC-6 ultra-microtome and imaged with a JEOL 1200EX electron microscope. For semi-thin sections, the samples were stained with I_2-KI and observed under a light microscope. In wheat, we focused on the endosperm cells on the crease side of the grain. For all analyses, three biological replicates were observed for each line.

For scanning electron microscopy (SEM), mature grains were dried at 37°C for one week, followed by fracturing to produce natural cross-sections. The samples were coated with gold using vacuum deposition and subsequently imaged with a Hitachi S-3400 scanning electron microscope (Hitachi, Japan). In wheat, we focused on the endosperm cells on the crease side of the mature grains. For all analyses, we observed six biological replicates per line. To assess the diameter of A-type starch granules, we quantified the fully visible granules in the images collected from six biological replicates, resulting in a total of 100 starch granules counted.

Grain composition measurement

Harvested wheat and rice grains were ground and sifted through a 100 μm mesh sieve to produce flour. Total starch content (six biological replicates) was quantified using a starch assay kit (Megazyme, Ireland), while amylose content (three biological replicates) was determined following the standard method (GB/T 15683-2008). The crude protein content in rice (three biological replicates) was assessed using the Kjeldahl method (ISO 20483:2013 (E)).

Statistics

Statistical analyses were performed using SPSS software. A two-tailed Student's *t*-test was used to assess differences between two groups. One-way ANOVA was applied to evaluate differences among multiple groups.

Data availability

The RNA-seq and DAP-seq data have been deposited in the National Center for Biotechnology Information (NCBI) (https://www.ncbi.nlm.nih.gov/) database under accession number PRJNA1275036.

FUNDING

This study was founded the Key national R&D program of China (2023YFF1000403, 2022YFD1201503), and the National Natural Science Foundation of China (32472143).

AUTHOR CONTRIBUTIONS

X.Y.Z., C.Y.H. and X.L. conceived and supervised the project. Y.C.L. performed most of the experiments. M.M.W. prepared the figures and tables included in the manuscript. M.M.W., Y.J.W. and J.H. performed some of the experiments. H.X.L. conducted the

GWAS. W.X. analyzed DAP-sequencing data. X.L.W., H.F.L., L.Z., T. L. and H.X. L. investigated the agronomic phenotypes. Y.C.L. and M.M.W. wrote the manuscript. D.S., X.Y.Z. and C.Y.H. revised the manuscript.

ACKNOWLEDGMENTS

We would like to thank Professor Genying Li (Shandong Academy of Agricultural Sciences) for assistance with wheat transformation. We would like to thank Professor Yangdong Guo (College of Horticulture, China Agricultural University) for kindly providing the GFP-nLUC and GFP-cLUC vectors. We also thanks to Professor Cristobal Uauy (John Innes Centre), Professor Wenhao Yan and Wei Chen, Dr. Chao He (Huazhong Agricultural University) for their valuable suggestions to the work.

DECLARATION OF INTERESTS

The authors declare no competing interest.

REFERENCES

Akihiro, T., Mizuno, K., and Fujimura, T. (2005). Gene expression of ADP-glucose pyrophosphorylase and starch contents in rice cultured cells are cooperatively regulated by sucrose and ABA. Plant Cell Physiol. **46**: 937-946. 10.1093/pcp/pci101.

Borrill, P., Ramirez-Gonzalez, R., and Uauy, C. (2016). expVIP: a Customizable RNA-seq Data Analysis and Visualization Platform. Plant Physiol. **170**: 2172-2186. 10.1104/pp.15.01667.

Cao, Y., Han, Z., Zhang, Z., He, L., Huang, C., Chen, J., Dai, F., Xuan, L., Yan, S., Si, Z., et al. (2024). UDP-glucosyltransferase 71C4 controls the flux of phenylpropanoid metabolism to shape cotton seed development. Plant Commun. **5**: 100938. 10.1016/j.xplc.2024.100938.

Cheng, S., Feng, C., Wingen, L., Cheng, H., Riche, A., Jiang, M., Waite, M.L., Huang, Z., Collier, S., Orford, S., et al. (2024). Harnessing landrace diversity empowers wheat breeding. Nature. **632**: 823-831. 10.1038/s41586-024-07682-9.

Chen, J., Watson-Lazowski, A., Kamble, N.U., Vickers, M., and Seung, D. (2023). Gene expression profile of the developing endosperm in durum wheat provides insight into starch biosynthesis. BMC Plant Biol. **23**: 363. 10.1186/s12870-023-04369-7.

Chen, J., Huang, B., Li, Y., Du, H., Gu, Y., Liu, H., Zhang, J., and Huang. Y. (2021).

Synergistic influence of sucrose and abscisic acid on the genes involved in starch synthesis in maize endosperm. Carbohydr. Res. **346**: 1684-1691. 10.1016/j.carres.2011.05.003.

Chen, J., Zhao, L., Li, H., Yang, C., Lin, X., Lin, Y., Zhang, H., Zhang, M., Bie, X., Zhao, P., et al. (2024). Nuclear factor-Y–polycomb repressive complex2 dynamically orchestrates starch and seed storage protein biosynthesis in wheat. Plant Cell. **35**: 4786-4803. 10.1093/plcell/koae256.

Chen, Y., Yan, Y., Wu, T.T., Zhang, G.L., Yin, H., Chen, W., Wang, S., Chang, F., and Gou, J.Y. (2020). Cloning of wheat keto-acyl thiolase 2B reveals a role of jasmonic acid in grain weight determination. Nat. Commun. **11**: 6266. 10.1038/s41467-020-20133-z.

Chourey, P.S., Taliercio, E.W., Carlson, S.J., and Ruan, Y.L. (1998). Genetic evidence that the two isozymes of sucrose synthase present in developing maize endosperm are critical, one for cell wall integrity and the other for starch biosynthesis. Mol. Gen. Genet. **259**: 88-96. 10.1007/s004380050792.

Dai, D., Mudunkothge, J.S., Galli, M., Char, S.N., Davenport, R., Zhou, X., Gustin, J.L., Spielbauer, G., Zhang, J., Barbazuk, W.B., et al. (2022). Paternal imprinting of dosage-effect defective1 contributes to seed weight xenia in maize. Nat. Commun. **13**: 5366. 10.1038/s41467-022-33055-9.

Deng, Y., Wang, J., Zhang, Z., and Wu, Y. (2020). Transactivation of *Sus1* and *Sus2* by Opaque2 is an essential supplement to sucrose synthase-mediated endosperm filling in maize. Plant Biotechnol. J. **18**: 1897-1907. 10.1111/pbi.13349.

Dong, N.Q., Sun, Y., Guo, T., Shi, C.L., Zhang, Y.M., Kan, Y., Xiang, Y.H., Zhang, H., Yang, Y.B., Li, Y.C., et al. (2020). UDP-glucosyltransferase regulates grain size and abiotic stress tolerance associated with metabolic flux redirection in rice. Nat. Commun. **11**: 2629. 10.1038/s41467-020-16403-5.

Dubos, C., Stracke, R., Grotewold, E., Weisshaar, B., Martin, C., and Lepiniec, L. (2010). MYB transcription factors in Arabidopsis. Trends Plant Sci. **15**: 573-581. 10.1016/j.tplants.2010.06.005.

Elbein, A.D., Pan, Y.T., Pastuszak, I., and Carroll, D. (2003). New insights on

763 trehalose: a multifunctional molecule. Glycobiology **13**: 17R-27R.
764 10.1093/glycob/cwg047.
765 **Emes, M.J., Bowsher, C.G., Hedley, C., Burrell, M.M., Scrase-Field, E.S., and**
766 **Tetlow, I.J.** (2003). Starch synthesis and carbon partitioning in developing endosperm.
767 J. Exp. Bot. **54**: 569-575. 10.1093/jxb/erg089.
768 **Fichtner, F., and Lunn, J.E.** (2021). The role of trehalose 6-phosphate (Tre6P) in plant
769 metabolism and development. Annu. Rev. Plant Biol. **72**: 737-760. 10.1146/annurev-
770 arplant-050718-095929.
771 **Fu, F.F., and Xue, H.W.** (2010). Coexpression analysis identifies rice starch regulator1,
772 a rice AP2/EREBP family transcription factor, as a novel rice starch biosynthesis
773 regulator. Plant Physiol. **154**: 927-938. 10.1104/pp.110.159517.
774 **Fujita, N., Toyosawa, Y., Utsumi, Y., Higuchi, T., Hanashiro, I., Ikegami, A.,**
775 **Akuzawa, S., Yoshida, M., Mori, A., Inomata, K., et al.** (2009). Characterization of
776 pullulanase (PUL)-deficient mutants of rice (*Oryza sativa* L.) and the function of PUL
777 on starch biosynthesis in the developing rice endosperm. J. Exp. Bot. **60**: 1009-1023.
778 10.1093/jxb/ern349.
779 **Gao, Y., An, K., Guo, W., Chen, Y., Zhang, R., Zhang, X., Chang, S., Rossi, V., Jin,**
780 **F., Cao, X., et al.** (2021). The endosperm-specific transcription factor TaNAC019
781 regulates glutenin and starch accumulation and its elite allele improves wheat grain
782 quality. Plant Cell **33**: 603-622. 10.1093/plcell/koaa040.
783 **Geng, Y., Pang, B., Hao, C., Tang, S., Zhang, X., and Li, T.** (2014). Expression of
784 wheat high molecular weight glutenin subunit *1Bx* is affected by large Insertions and
785 deletions located in the upstream flanking sequences. PLoS ONE **9**:
786 10.1371/journal.pone.0105363.
787 **Ghorbel, M., Brini, F., Sharma, A., and Landi, M.** (2021). Role of jasmonic acid in
788 plants: the molecular point of view. Plant Cell Rep. **40**: 1471-1494. 10.1007/s00299-
789 021-02687-4.
790 **Gu, Y., Han, S., Chen, L., Mu, J., Duan, L., Li, Y., Yan, Y., and Li, X.** (2021).
791 Expression and regulation of genes involved in the reserve starch biosynthesis pathway
792 in hexaploid wheat (*Triticum aestivum* L.). Crop J. **9**: 440-455.

10.1016/j.cj.2020.08.002.

Hao, C., Jiao, C., Hou, J., Li, T., Liu, H., Wang, Y., Zheng, J., Liu, H., Bi, Z., Xu, F., et al. (2020). Resequencing of 145 landmark cultivars reveals asymmetric sub-genome selection and strong founder genotype effects on wheat breeding in China. Mol. Plant **13**: 1733-1751. 10.1016/j.molp.2020.09.001.

Hou, J., Jiang, Q., Hao, C., Wang, Y., Zhang, H., and Zhang, X. (2014). Global selection on sucrose synthase haplotypes during a century of wheat breeding. Plant Physiol. **164**: 1918-1929. 10.1104/pp.113.232454.

Hu, Y., Li, Y., Weng, J., Liu, H., Yu, G., Liu, Y., Xiao, Q., Huang, H., Wang, Y., Wei, B., et al. (2021). Coordinated regulation of starch synthesis in maize endosperm by microRNAs and DNA methylation. Plant J. **105**: 108-123. 10.1111/tpj.15043.

Huang, L., Tan, H., Zhang, C., Li, Q., and Liu, Q. (2021). Starch biosynthesis in cereal endosperms: An updated review over the last decade. Plant Commun. **2**: 100237. 10.1016/j.xplc.2021.100237.

Jain, B.P., and Pandey, S. (2018). WD40 repeat proteins: Signalling scaffold with diverse functions. Protein J. 37: 391–406. 10.1007/s10930-018-9785-7.

James, M.G., Denyer, K., and Myers, A.M. (2003). Starch synthesis in the cereal endosperm. Curr. Opin. in Plant Biol. **6**: 215-222. 10.1016/s1369-5266(03)00042-6.

Jiang, C.K., and Rao, G.Y. (2020). Insights into the diversification and evolution of R2R3-MYB transcription factors in plants. Plant Physiol. **183**: 637-655. 10.1104/pp.19.01082.

Johnson, P.E., Patron, N.J., Bottrill, A.R., Dinges, J.R., Fahy, B.F., Parker, M.L., Waite, D.N., and Denyer, K. (2003). A low-starch barley mutant, *riso 16*, lacking the cytosolic small subunit of ADP-glucose pyrophosphorylase, reveals the importance of the cytosolic isoform and the identity of the plastidial small subunit. Plant Physiol. **131**: 684-696. 10.1104/pp.013094.

Kang, G.Z., Xu, W., Liu, G.-Q., Peng, X.-Q., Guo, T.-C., and Bell, J. (2013). Comprehensive analysis of the transcription of starch synthesis genes and the transcription factor *RSR1* in wheat (*Triticum aestivum*) endosperm. Genome **56**: 115-122. 10.1139/gen-2012-0146.

Kawakatsu, T., Yamamoto, M.P., Touno, S.M., Yasuda, H., and Takaiwa, F. (2009). Compensation and interaction between RISBZ1 and RPBF during grain filling in rice. Plant J. **59**: 908-920. 10.1111/j.1365-313X.2009.03925.x.

Li, E., Hasjim, J., Gilding, E.K., Godwin, I.D., Li, C., and Gilbert, R.G. (2019). The role of pullulanase in starch biosynthesis, structure, and thermal properties by studying *Sorghum* with increased pullulanase activity. Starch - Stärke **71**: 10.1002/star.201900072.

Li, H., Liu, H., Hao, C., Li, T., Liu, Y., Wang, X., Yang, Y., Zheng, J., and Zhang, X. (2023). The auxin response factor TaARF15-A1 negatively regulates senescence in common wheat (*Triticum aestivum* L.). Plant Physiol. **191**: 1254-1271. 10.1093/plphys/kiac497.

Li, J., Xie, L., Tian, X., Liu, S., Xu, D., Jin, H., Song, J., Dong, Y., Zhao, D., Li, G., et al. (2021). TaNAC100 acts as an integrator of seed protein and starch synthesis exerting pleiotropic effects on agronomic traits in wheat. Plant J. **108**: 829-840. 10.1111/tpj.15485.

Liu, H., Si, X., Wang, Z., Cao, L., Gao, L., Zhou, X., Wang, W., Wang, K., Jiao, C., Zhuang, L., et al. (2023a). *TaTPP-7A* positively feedback regulates grain filling and wheat grain yield through T6P-SnRK1 signalling pathway and sugar-ABA interaction. Plant Biotechnol. J. **21**: 1159-1175. 10.1111/pbi.14025.

Liu, Y., Hou, J., Wang, X., Li, T., Majeed, U., Hao, C., and Zhang, X. (2020). The NAC transcription factor NAC019-A1 is a negative regulator of starch synthesis in wheat developing endosperm. J. Exp. Bot. **71**: 5794-5807. 10.1093/jxb/eraa333.

Liu, Y., Xi, W., Wang, X., Li, H., Liu, H., Li, T., Hou, J., Liu, X., Hao, C., and Zhang, X. (2023b). TabHLH95-TaNF-YB1 module promotes grain starch synthesis in bread wheat. J. Genet. Genomics **50**: 883-894. 10.1016/j.jgg.2023.04.002.

Lopez-Gonzalez, C., Juarez-Colunga, S., Morales-Elias, N.C., and Tiessen, A. (2019). Exploring regulatory networks in plants: transcription factors of starch metabolism. PeerJ **7**: e6841. 10.7717/peerj.6841.

Love, M.I., Huber, W., and Anders, S. (2014). Moderated estimation of fold change and dispersion for RNA-seq data with DESeq2. Genome Biol. **15**: 10.1186/s13059-014-

0550-8.

Ma, B., Zhang, L., Gao, Q., Wang, J., Li, X., Wang, H., Liu, Y., Lin, H., Liu, J., Wang, X., et al. (2021). A plasma membrane transporter coordinates phosphate reallocation and grain filling in cereals. J. Integr. Plant Biol. **65**: 526-547. 10.1111/jipb.13456.

Ma, B., Zhang, L., and He, Z. (2023). Understanding the regulation of cereal grain filling: The way forward. Nat. Genet. **53**: 906-915. 10.1038/s41588-021-00855-6.

Mehra, P., Pandey, B.K., Verma, L., Prusty, A., Singh, A.P., Sharma, S., Malik, N., Bennett, M.J., Parida, S.K., Giri, J., and Tyagi, A.K. (2022). OsJAZ11 regulates spikelet and seed development in rice. Plant Direct **6**: e401. 10.1002/pld3.401.

Niaz, M., Zhang, L., Lv, G., Hu, H., Yang, X., Cheng, Y., Zheng, Y., Zhang, B., Yan, X., Htun, A., et al. (2023). Identification of *TaGL1-B1* gene controlling grain length through regulation of jasmonic acid in common wheat. Plant Biotechnol. J. **21**: 979-989. 10.1111/pbi.14009.

Niu, B., Deng, H., Li, T., Sharma, S., Yun, Q., Li, Q., E, Z., and Chen, C. (2020). OsbZIP76 interacts with OsNF-YBs and regulates endosperm cellularization in rice (*Oryza sativa*). J. Integr. Plant Biol. **62**: 1983-1996. 10.1111/jipb.12989.

Ostrowski, M., and Jakubowska, A. (2014). Udp-glycosyltransferases of plant hormones. Adv. in Cell Biol. **4**: 43-60. 10.2478/acb-2014-0003.

Paul, M.J., Watson, A., and Griffiths, C.A. (2020). Trehalose 6-phosphate signalling and impact on crop yield. Biochem. Soc. Trans. **48**: 2127-2137. 10.1042/bst20200286.

Pei, H., Teng, W., Gao, L., Gao, H., Ren, X., Liu, Y., Jia, J., Tong, Y., Wang, Y., and Lu, Z. (2023). Low-affinity SPL binding sites contribute to subgenome expression divergence in allohexaploid wheat. Sci. China Life Sci. **66**: 819-834. 10.1007/s11427-022-2202-3.

Ramsay, N.A., and Glover, B.J. (2005). MYB-bHLH-WD40 protein complex and the evolution of cellular diversity. Trends Plant Sci. **10**: 63-70. 10.1016/j.tplants.2004.12.011.

Ross, J., Li, Y., Lim, E., and Bowles, D.J. (2001). Higher plant glycosyltransferases. Genome Biol. **2**: 3004. 10.1186/gb-2001-2-2-reviews3004.

Shannon, J.C., Pien, F.M., Cao H.P., and Liu K.C. (1998). Brittle-1, an adenylate translocator, facilitates transfer of extraplastidial synthesized ADP-glucose into amyloplasts of maize endosperms. Plant Physiol. **177**: 1235-1252. doi.org/10.1104/pp.117.4.1235.

Shen, L., Zhang, L., Yin, C., Xu, X., Liu, Y., Shen, K., Wu, H., Sun, Z., Wang, K., He, Z., et al. (2024). The wheat sucrose synthase gene *TaSus1* is a determinant of grain number per spike. Crop J. **12**: 295-300. 10.1016/j.cj.2023.11.007.

Shevkani, K., Singh, N., Bajaj, R., and Kaur, A. (2016). Wheat starch production, structure, functionality and applications—a review. Int. J. Food Sci. Technol. **52**: 38-58. 10.1111/ijfs.13266.

Song, Y., Luo, G., Shen, L., Yu, K., Yang, W., Li, X., Sun, J., Zhan, K., Cui, D., Liu, D., and Zhang, A. (2020). *TubZIP28*, a novel bZIP family transcription factor from *Triticum urartu*, and *TabZIP28*, its homologue from *Triticum aestivum*, enhance starch synthesis in wheat. New Phytol. **226**: 1384-1398. 10.1111/nph.16435.

Stracke, R., Werber, M., and Weisshaar, B. (2001). The R2R3-MYB gene family in *Arabidopsis thaliana*. Curr. Opin. in Plant Biol. **4**: 447-456. 10.1016/S1369-5266(00)00199-0.

Tian, T., Liu, Y., Yan, H., You, Q., Yi, X., Du, Z., Xu, W., and Su, Z. (2017). agriGO v2.0: a GO analysis toolkit for the agricultural community, 2017 update. Nucleic Acids Res. **45**: W122-W129. 10.1093/nar/gkx382.

Tsai, C.Y., and Nelson, O.E. (1966) Starch-deficient maize mutant lacking adenosine diphosphate glucose pyrophophorylase activity. Science **151**: 341-343.

Uauy, C., Paraiso, F., Colasuonno, P., Tran, R.K., Tsai, H., Berardi, S., Comai, L., and Dubcovsky, J. (2009). A modified TILLING approach to detect induced mutations in tetraploid and hexaploid wheat. BMC Plant Biol. **9**: 115. 10.1186/1471-2229-9-115.

Wang, F., Yang, F., Zhu, D., Saniboere, B., Zhou, B., and Peng, D. (2024) MYB44 plays key roles in regulating plant responses to abiotic and biotic stress, metabolism, and development. J. Plant Biochem. Biotechnol. **33**: 462–473. 10.1007/s13562-023-00864-y.

Wang, H., Huang, Y., Li, Y., Cui, Y., Xiang, X., Zhu, Y., Wang, Q., Wang, X., Ma,

G., Xiao, Q., et al. (2024a). An ARF gene mutation creates flint kernel architecture in dent maize. Nat. Commun. 15: 2565. 10.1038/s41467-024-46955-9.

Wang, J., Chen, Z., Zhang, Q., Meng, S., and Wei, C. (2020). The NAC transcription factors OsNAC20 and OsNAC26 regulate starch and storage protein synthesis. Plant Physiol. **184**: 1775-1791. 10.1104/pp.20.00984.

Wang, J., Zhang, H., Wang, Y., Meng, S., Liu, Q., Li, Q., Zhao, Z., Liu, Q., and Wei, C. (2024b). Regulatory loops between rice transcription factors OsNAC25 and OsNAC20/26 balance starch synthesis. Plant Physiol. **195**: 1365-1381. 10.1093/plphys/kiae139.

Wang, X., Liu, Y., Hao, C., Li, T., Majeed, U., Liu, H., Li, H., Hou, J., and Zhang, X. (2023). Wheat NAC-A18 regulates grain starch and storage proteins synthesis and affects grain weight. Theor. Appl. Genet. **136**: 123. 10.1007/s00122-023-04365-3.

Wang, Y., Hou, J., Liu, H., Li, T., Wang, K., Hao, C., Liu, H., and Zhang, X. (2019). *TaBT1*, affecting starch synthesis and thousand kernel weight, underwent strong selection during wheat improvement. J. Exp. Bot. 70: 1497-1511. 10.1093/jxb/erz032.

Xiang, D., Quilichini, T.D., Liu, Z., Gao, P., Pan, Y., Li, Q., Nilsen, K.T., Venglat, P., Esteban, E., Pasha, A., et al. (2019). The transcriptional landscape of polyploid wheats and their diploid ancestors during embryogenesis and grain development. Plant Cell **31**: 2888-2911. 10.1105/tpc.19.00397.

Zhang, Z., Dong, J., Ji, C., Wu, Y., and Messing, J. (2019). NAC-type transcription factors regulate accumulation of starch and protein in maize seeds. Proc. Natl. Acad. Sci. U.S.A. **116**: 11223-11228. 10.1073/pnas.1904995116.

Zhang, Z., Zheng, X., Yang, J., Messing, J., and Wu, Y. (2016). Maize endosperm-specific transcription factors O2 and PBF network the regulation of protein and starch synthesis. Proc. Natl. Acad. Sci. U.S.A. **113**: 10842-10847. 10.1073/pnas.1613721113.

Zhou, X., and Stephens, M. (2012). Genome-wide efficient mixed-model analysis for association studies. Nat. Genet. **44**: 821-824. 10.1038/ng.2310.

Zhu, T., Wang, L., Rimbert, H., Rodriguez, J.C., Deal, K.R., De Oliveira, R., Choulet, F., Keeble-Gagnere, G., Tibbits, J., Rogers, J., et al. (2021). Optical maps refine the bread wheat *Triticum aestivum* cv. Chinese Spring genome assembly. Plant J.

943 **107**: 303-314. 10.1111/tpj.15289.

FIGURE LEGENDS

Figure 1. *TaMYB44-A1* haplotypes are associated with total starch content in wheat. (A) Results of the GWAS for grain total starch content (TSC). The horizontal dashed line represents the genome-wide suggestive significance threshold ($P = 1.0\times10^{-5}$). (B) Quantile-quantile plot for the GWAS under the mixed linear model. **(C)** Manhattan plot and linkage disequilibrium heatmap surrounding the associated peak for total starch content on chromosome 4A. The black dashed lines indicate the candidate genomic region. The region is zoomed in, then lines represent the positions of the 10 candidate genes, and then *TaMYB44-A1* is marked in red. **(D)** Tissue expression heatmap of candidate genes at the *qTSC4A* locus. The candidate gene is highlighted in red. Data sourced from the Wheat Expression Database. **(E)** Allelic variation in the coding sequence (CDS) of *TaMYB44-A1*. Red represents the alleles that causes the amino acid change. **(F)** Accessions harboring *TaMYB44-A1-Hap2* exhibited higher total starch content compared to those with *Hap1*. Data were analyzed using a two-tailed Student's *t* test (**$P < 0.01$).

Figure 2. *TaMYB44* negatively regulates starch synthesis and grain weight. Total starch content (**A**) and starch content per grain (**B**) in WT and *TaMYB44* transgenic lines (OE and KO), based on six biological replicates. (**C**) Diameter of A-type starch granules. The diameter of A-type starch granules was assessed by measuring a total of 100 granules sampled across six biological replicates. **(D)** Starch granules in the developing wheat endosperm at 12 DAP (n = three biological replicates), Scale bar = 20 μm. **(E)** Scanning electron microscope imaging of the crease area in mature grains from WT, *TaMYB44*-OE, and *Tamyb44*-KO lines. n = six biological replicates, Scale bars = 20 μm. **(F)** Representative grains from WT and *TaMYB44* transgenic lines, with a scale bar of 1cm. Grain length (**G**), grain width (**H**), thousand grain weight (**I**) and grain yield per plant (**J**) of WT, *Tamyb44*-KO and *TaMYB44*-OE measured in single-row growth conditions (no less than 50 individual plants were measured). (**K**) Grain yield per plot (n = 6). One-way ANOVA was employed to analyze the data (*$P < 0.05$, **$P < 0.01$).

Figure 3. Pathways and downstream genes regulated by TaMYB44. (A) The

TaMYB44-binding motif and its reverse complementary motif identified through DAP-Seq analysis. **(B)** A Venn diagram showing the number of overlapping genes in transcriptome and DAP-seq. **(C)** GO enrichment analysis of the upregulated-DEGs in the *Tamyb44*-KO lines. **(D)** TaMYB44 directly binds to the promoter of downstream genes, as validated by DAP-seq. **(E)** EMSA assay verifying the interaction between TaMYB44 and the promoters of downstream gene. **(F)** Y1H assay validating the interaction between TaMYB44 and downstream gene promoters. **(G)** TaMYB44 decreases the transcriptional activity of the *TaLD-B1*, *TaTPP-D1*, *TaUGT83A1-B1*, and *TaUGT83A1-D1* promoters. Error bars indicate the standard deviation (± SD) of five biological replicates (two-tailed Student's *t*-test, $^{**}P < 0.01$).

Figure 4. TaMYB44 negatively regulates starch and JA accumulation by repressing the expression of *TaUGT83A1*. (A) Heatmap showing the expression levels of JA-related genes in Fielder (WT) and *Tamyb44*-KO lines. The color scale represents the $\log_2$-fold change in FPKM ratios, with the FPKM value in the Fielder background normalized to one. **(B)** Quantification of JA and its derivatives in Fielder and *Tamyb44*-KO developing grains. Statistical significance was assessed using a two-tailed Student's *t*-test ($^{*}P < 0.05$, $^{**}P < 0.01$). **(C)** Schematic diagram illustrating the null mutants of *TaUGT83A1* homologs. **(D)** *Taugt83a1* mutants exhibit smaller grain size compared to Kronos. Scale bar = 1 cm. **(E-I)** Total starch content (n = 6) **(E)**, Grain length (**F**), grain width (**G**), thousand grain weight (**H**), and grain yield per plant (**I**) of *Taugt83a1* mutants and Kronos under single-row grown conditions. For **E-I**, data were presented as means ± S.D. ($n \geqslant 15$), and statistical analysis was conducted using one-way ANOVA ($^{*}P < 0.05$, $^{**}P < 0.01$).

Figure 5. TaWDR1 interacts with TaMYB44 and mitigates its negative impact on starch synthesis and grain weight. (A) TaWDR1 and TaMYB44 co-localized in the nucleus. Scale bar = 10 μm. **(B)** Y2H confirming the interaction between TaMYB44 and TaWDR1. AD, activation domain; BD, binding domain. -LWHA means plates without Trp, Leu, His, and Ade. **(C)** Co-IP assay demonstrating the interaction between TaMYB44 and TaWDR1. **(D)** Representative grains of WT and three *TaWDR1*-OE lines

showing differences in grain width. Scale bar = 1cm. **(E)** Transcript levels of *TaWDR1* in WT and *TaWDR1*-OE lines. *TaActin* as an internal control. Data represented as mean ± S.D., and statistical analysis was conducted using one-way ANOVA (**$P < 0.01$). **(F)** Total starch content in WT and *TaWDR1*-OE lines. *TaWDR1-D1*-OE increased grain width **(G)** and thousand grain weight **(H)** in Fielder wheat. For panels **F-H**, data came from no less than 20 individual plants, and statistical analysis was performed using one-way ANOVA (*$P < 0.05$, **$P < 0.01$). **(I)** Starch granules in the 15 DAP developing endosperm of WT, *TaMYB44*-OE, *TaWDR1*-OE, and their F_3 generations. Scale bar = 20 μm. **(J)** Representative grains of *TaMYB44*-OE, *TaWDR1*-OE, and their F_3 generations, Scale bar = 1 cm. Total starch content (n = 6) **(K)**, Grain width **(L)** and thousand grain weight **(M)** of WT, *TaMYB44*-OE, *TaWDR1*-OE, and their F_3 generations. For panels **L-M**, data represent measurements from more than 25 individual plants. Statistical analysis for panels **K-M** was performed using one-way ANOVA, with lowercase letters indicating significance at $P < 0.05$.

Figure 6. *MYB44* negatively regulates starch accumulation and grain weight in rice. Total starch content (n = 6) (**A**), Amylose content (n = 3) (**B**) and total protein content (n = 3) (**C**) in the grains of Kitaake and *p1Bx7::TaMYB44* rice lines. Differences were analyzed using one-way ANOVA (**$P < 0.01$). **(D)** Morphology of starch granules in the mature endosperm of Kitaake and *p1Bx7::TaMYB44* lines. White scale = 1 mm, red scale = 100 μm. **(E)** Iodine-potassium iodide staining shows starch content in the developing endosperm of Kitaake and *p1Bx7::TaMYB44* rice lines. DAP represents days after pollination. Scale bar = 50 μm. **(F)** Morphology of starch granule complex in the developing endosperm of Kitaake and *p1Bx7::TaMYB44* rice lines. Developing grains from Kitaake and *p1Bx7::TaMYB44* rice lines were sampled at 8 DAP for TEM observation (n = 3 biological replicates). Scale bar = 10 μm. Thousand grain weight (**G**), and gain yield per plant (**H**) were measured over two environments. For panels **G** and **H**, data represent measurements from more than 15 individual plants. Statistical significance was assessed using one-way ANOVA (**$P < 0.01$). **(I)** KEGG analysis of down-regulated differentially expressed genes in *p1Bx7::TaMYB44* rice grains at 8 and 12 DAP.

Figure 7. Proposed model of *TaMYB44* function in regulating starch synthesis and grain weight. This working model shows that TaMYB44 negatively regulates starch synthesis and grain weight by modulating three pathways, including jasmonic acid (JA) biosynthesis (indirectly), trehalose metabolism, and starch biosynthesis pathways. TaWDR1 interacts with TaMYB44 and functions as a modulator that counteract the repressive effects of TaMYB44.

SUPPLEMENTARY INFORMATION

Supplementary Figure 1. *TaMYB44* encodes a nuclear-localized transcription factor.

Supplementary Figure 2. Phenotypes of *TaMYB44* OE and KO lines.

Supplementary Figure 3. Pathways and downstream genes regulated by TaMYB44.

Supplementary Figure 4. Trehalose synthesis of *Tamyb44* triple KO mutants.

Supplementary Figure 5. TaMYB44 interacting proteins and interaction validation.

Supplementary Figure 6. TaWDR1 interacts with TaMYB44 to alleviate the inhibitory effect of TaMYB44 on starch synthesis.

Supplementary Figure 7. Functional conservation of *TaMYB44* in rice.

Supplementary Figure 8. *OsMYB44* negatively regulates starch synthesis and grain weight in rice.

Supplementary Figure 9. The expression level of starch synthesis-related genes in KitaaKe (WT), *p1Bx7::TaMYB44* rice lines, and *p1Bx7::OsMYB44* rice lines.

Supplementary Figure 10. Haplotype distribution of *TaMYB44-A1* and its association with thousand grain weight in wheat populations.

Supplementary Figure 11. Expression and functional assessment of *TaMYB44-A1* haplotypes.

Supplementary Table 1. Genes in the *qTSC4A* LD block.

Supplementary Table 2. The agronomic traits of *TaMYB44* transgenic lines and WT in single-row growing conditions

Supplementary Table 3. List of TaMYB44 interacting proteins identified by Y2H screening.

Supplementary Table 4. The agronomic traits of *pUBI::TaWDR1-D1* wheat lines in single-row growing conditions

Supplementary Table 5. The agronomic traits of *TaMYB44*-OE/*TaWDR1*-OE F3 generations in single-row growing conditions.

Supplementary Data 1. Differentially expressed genes and GO enrichment of *TaMYB44*-OE, *Tamyb44* triple KO vs WT (Fielder).

Supplementary Data 2. Differential metabolites in developing grains of *Tamyb44* triple KO and Fielder wheat at 12 and 16 DAP.

Supplementary Data 3. Differentially expressed genes and KEGG results of *p1Bx7::TaMYB44* rice vs WT (Kitaake).

Supplementary Data 4. List of primers used in this study.